EUKARYOTIC CELL, Apr. 2008, p. 698–711 Vol. 7, No. 4
1535-9778/08/$08.00+0 doi:10.1128/EC.00021-08

MORN1 Has a Conserved Role in Asexual and Sexual Development across the Apicomplexa▽

David J. P. Ferguson,[1] Nivedita Sahoo,[2] Robert A. Pinches,[3] Janene M. Bumstead,[4] Fiona M. Tomley,[4] and Marc-Jan Gubbels[2]*

Nuffield Department of Pathology, University of Oxford, John Radcliffe Hospital, Oxford OX3 9DU, United Kingdom[1]; Department of Biology, Boston College, Chestnut Hill, Massachusetts[2]; Nuffield Department of Medicine, Molecular Parasitology, Weatherall Institute of Molecular Medicine, University of Oxford, John Radcliffe Hospital, Oxford OX3 9DS, United Kingdom[3]; and Division of Microbiology, Institute for Animal Health, Compton, Newbury, Berkshire RG20 7NN, United Kingdom[4]

Received 16 January 2008/Accepted 21 February 2008

The gene encoding the membrane occupation and recognition nexus protein MORN1 is conserved across the Apicomplexa. In *Toxoplasma gondii*, MORN1 is associated with the spindle poles, the anterior and posterior rings of the inner membrane complex (IMC). The present study examines the localization of MORN1 during the coccidian development of *T. gondii* and three *Eimeria* species (in the definitive host) and erythrocytic schizogony of *Plasmodium falciparum*. During asexual proliferation, MORN1 is associated with the posterior ring of the IMCs of the multiple daughters forming during *T. gondii* endopolygeny and schizogony in *Eimeria* and *P. falciparum*. Furthermore, the expression of *P. falciparum* MORN1 protein peaked in late schizogony. These data fit a model with a conserved role for MORN1 during IMC assembly in all variations of asexual development. An important new observation is the reactivity of MORN1 antibody with certain sexual stages in *T. gondii* and *Eimeria* species. Here MORN1 is organized as a ring-like structure where the microgametes bud from the microgametocyte while in mature microgametes it is present near the flagellar basal bodies and mitochondrion. These observations suggest a conserved role for MORN1 in both asexual and sexual development across the Apicomplexa.

Protozoan parasites of the phylum Apicomplexa cause many diseases that interfere with human well-being. Several diseases affect humans directly, for example malaria (*Plasmodium* species), toxoplasmosis (*Toxoplasma gondii*), and cryptosporidiosis (*Cryptosporidium parvum*), whereas various parasites (*Eimeria*, *Theileria*, *Babesia*, and *Sacrocystis* species plus *Neospora caninum* and *T. gondii*) can affect domestic animals. The life cycles of apicomplexan parasites are extremely variable, employing various methods of transmission between hosts, which can involve direct transmission (the fecal/oral route, e.g., *Eimeria* species), insect vectors (e.g., *Plasmodium*, *Theileria*, and *Babesia* species), intermediate hosts (e.g., the cyst-forming Coccidia, such as *T. gondii*), or vertical transmission (mother to offspring, e.g., *N. caninum* and *T. gondii*). In all cases, the life cycle involves both asexual and sexual development and, as obligate intracellular parasites, most of this development occurs within the confines of host cells.

Within the Apicomplexa, there have been numerous studies of both asexual and sexual development, but this has been limited to morphological studies of in vivo development with the exception of the few parasite stages that can be maintained in culture. In the case of asexual division, the start and end points are always the same: an (increased number of) invasion-competent motile "zoite" (Fig. 1). However, ultrastructural studies have identified four variations of the asexual process related to differences in the number and timing of DNA replication and nuclear division and the location of daughter formation, which result in distinctive morphological features (11, 14, 30, 35, 38, 40) summarized in Fig. 1. The vast majority of species in all genera of the Apicomplexa undergo a process termed schizogony in which large numbers (ranging from 16 to many hundreds) of daughters are formed simultaneously from one invading zoite. The process involves repeated cycles of DNA replication and nuclear division, giving rise to a multinucleated stage, followed by daughter cell formation, which is associated with budding from the surface of the mother cell (Fig. 1). However, within a subgroup of the Coccidia, termed the cyst-forming Coccidia, three additional processes can be identified (Fig. 1). All three processes differ from schizogony in that daughter formation takes place within the mother cell cytoplasm, but the processes differ from each other in the number of DNA replication cycles and timing of nuclear division (Fig. 1). The terms schizogony, endodyogeny, *Toxoplasma* endopolygeny for the process undergone by *T. gondii* in the definite host, and *Sarcocystis* endopolygeny for that undergone by *Sarcocystis* species in the intermediate host were proposed previously (reviewed in reference 14).

The most extensively studied division process is the simplest form, endodyogeny, undergone by the tachyzoite of *T. gondii* in which two daughters are formed (15, 16, 18, 19, 31, 35, 39). One of the earliest steps in endodyogeny is the duplication of the centrosome (16, 31, 39), which appears to provide the spatial nucleation cue for the development of two new daughter cytoskeleton scaffolds (15, 18, 19). The new scaffolds develop into cone-shaped structures with the open end always directed toward the nuclear poles/centrosome (15, 22, 29, 35). These daughter cytoskeletal scaffolds are composed of a com-

* Corresponding author. Mailing address: Department of Biology, Boston College, 140 Commonwealth Avenue, 355 Higgins Hall, Chestnut Hill, MA. Phone: (617) 552-8722. Fax: (617) 552-2011. E-mail: gubbelsj@bc.edu.

▽ Published ahead of print on 29 February 2008.

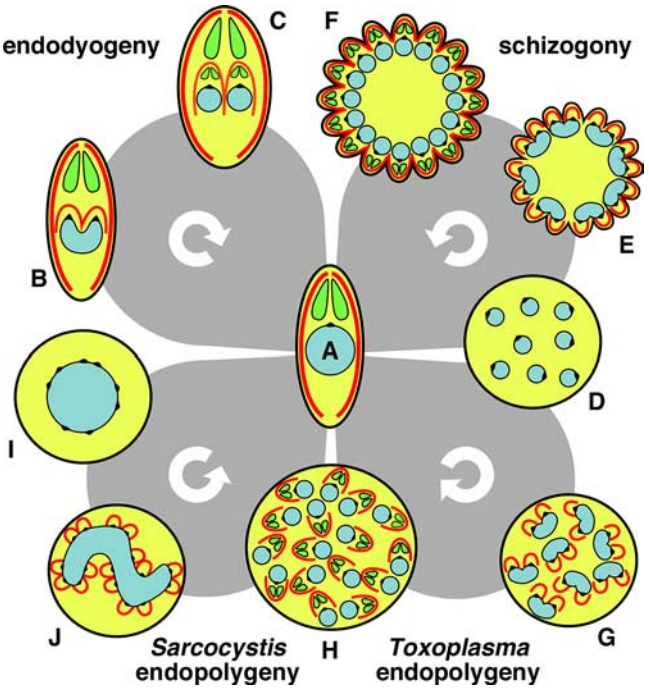

FIG. 1. Apicomplexan cell division flexibility. (A) The beginning and end product of division is the host cell invasion-competent "zoite." Endodyogeny (A to C) is the formation of two daughters through internal budding. In schizogony (A and D to F), parasites first go through multiple rounds of DNA replication and mitosis before budding and this is set apart from other strategies in that budding takes place at the plasma membrane. Division by endopolygeny, as carried out by *T. gondii* in the cat gut (A, D, G, and H), also involves multiple rounds of DNA replication and mitosis, but budding takes place internally within the cytoplasm. Endopolygeny, as undergone by *Sarcocystis neurona* (A and H to J), goes through several rounds of DNA replication but omits karyokineses, and budding takes place internally within the cytoplasm. Daughter cell budding in schizogony and both forms of endodyogeny is dependent on a final round of DNA replication and mitosis and, in this last round, is very reminiscent of endodyogeny. The nucleus is shown in light blue, the cytoskeleton is shown in red (IMC-positive subpellicular microtubules), and apical rhoptry organelles are presented in green. The black "knobs" on the nucleus represent the spindle pole/centriolar complex.

bination of flattened vesicles and intermediate filaments with underlying microtubules, collectively known as the inner membrane complex (IMC). The IMC grows posteriorly and forms a scaffold for new organelle assembly and segregation (19, 40). Finally, the mother's cytoskeleton is disassembled and the mother cell plasma membrane encloses the emerging daughters. In a recent study, it was shown that the protein TgMORN1 is associated with endodyogeny (15). With the use of an antibody to recombinant TgMORN1, it has previously been shown that the protein was located in the nuclear pole and the free ends of the IMC, with weak staining of the anterior polar ring and stronger staining of the posterior ring of the mature tachyzoite (15). During endodyogeny, the protein was prominently associated with the open end of the daughter IMC as it grew posteriorly (15). Therefore, the first question investigated in the present study was whether MORN1 played a similar role in *Toxoplasma* endopolygeny during coccidian development. This matter was examined during asexual development within the small intestine of the cat by using immunocytochemistry. In addition, MORN1 homologues are conserved in a number of apicomplexan species (15), which raises the question of a possible conserved role for MORN1 during development across the Apicomplexa. The present study was extended to examine asexual development during schizogony of *Eimeria tenella*, *Eimeria acervulina*, and *Eimeria maxima* in the ceca and small intestines of the chicken and *Plasmodium falciparum* within in vitro-cultured erythrocytes.

With the exception of *Plasmodium* species, where the sexual stages can be observed in the insect blood meal or the process of gamete development can be stimulated in vitro, our knowledge of sexual development has almost exclusively been limited to in vivo morphology and a few immunohistological studies (23, 37). To date, the sexual stages of all coccidian parasites have proven refractile to cell-culturing techniques, which has made applying modern molecular techniques difficult. Within the Coccidia, sexual development involves the formation of distinctive micro- and macrogametes that fuse to form a zygote. The zygote is the only diploid stage and immediately undergoes meiotic division, making all the asexual stages haploid. Within the definitive host, after a number of asexual cycles, merozoites entering new host cells can develop into either microgametocytes or macrogametocytes rather than undergoing another round of asexual proliferation. Since the parasite is haploid and there are no sex chromosomes, this development must represent a phenotypic change. However, the factors controlling the conversion to sexual development and the factors controlling whether a merozoite will develop into a micro- or macrogametocyte are unknown. The microgametocyte gives rise to a number (ranging from 30 to many hundreds) of microgametes, which bud from the surface of the mother cell (7, 11, 33). The motile microgametes are unique within the coccidian life cycle in possessing flagella. In contrast, macrogametogony involves an increase in size, but no nuclear division, and the synthesis of material required for oocyst wall formation (wall-forming bodies) and storage (polysaccharide granules and lipid droplets) to allow the mature macrogamete to develop into the oocyst and undergo sporulation in the external environment (8, 12, 34). In the present study, while examining the asexual development in the definitive host, we also examined the expression of MORN1 during sexual development in *T. gondii* and in the three species of *Eimeria*. An unexpected finding was the observation that MORN1 was involved with the budding process during microgamete formation and was also present within the mature microgamete. Thus, MORN1 appears to play a conserved, possibly structural role in both asexual and sexual development.

MATERIALS AND METHODS

Parasites. (i) *T. gondii*. The coccidian stages of *T. gondii* were examined in the small intestines of cats as described previously (9).

(ii) *E. tenella*, *E. acervulina*, and *E. maxima*. Samples of small intestine (*E. maxima* and *E. acervulina*) or cecum (*E. tenella*) were taken from chickens autopsied at various intervals postinfection by using a technique described previously (14).

(iii) *P. falciparum*. The process of schizogony was examined in the A4 strain of *P. falciparum* grown in human erythrocytes by using techniques described previously (42).

Antibodies. (i) Anti-TgMORN1. Anti-TgMORN1 is an affinity-purified rabbit antibody against the recombinant membrane occupation and recognition nexus protein 1 (MORN1) of *T. gondii* (15).

(ii) Anti-TgIMC1. Anti-TgIMC1 is a monoclonal mouse antibody that recognizes the *T. gondii* IMC protein 1 (IMC1) (26) (kindly provided by Gary Ward, University of Vermont).

(iii) Anti-TgENO2. Anti-TgENO2 is a mouse antibody that recognizes the enolase 2 (ENO2) isoform of *T. gondii*, which weakly stains the cytoplasm and strongly stains the nuclei in actively developing parasites (13) (kindly provided by Stan Tomavo, Universite des Sciences et Technologies de Lille, France).

(iv) Anti-TgENR. Anti-TgENR is a mouse antibody that recognizes the enoyl reductase (ENR) of *T. gondii*, which is located in the apicoplast (10).

(v) Anti-TgGRA7. Anti-TgGRA7 is a mouse monoclonal antibody to the dense granule protein 7 (GRA7) (20) that stains the parasitophorous vacuole and the dense granules within the merozoites (9) (kindly provided by D. Jacobs, Innogenetics NV, Belgium).

(vi) Anti-EtENR. Anti-EtENR is a mouse antibody to *E. tenella* ENR, which identifies the apicoplast in *Eimeria* species (14).

(vii) Anti-EtAMA2. Anti-EtAMA2 is protein that recognizes the apical membrane antigen 2 protein (AMA2) that is located in the micronemes of the merozoites of *E. tenella* (F. Tomley, unpublished data).

(viii) Anti-EmAPGA. Anti-EmAPGA is a protein raised against affinity-purified gametocyte antigens (APGA) of *E. maxima* that recognizes the wall-forming bodies within the macrogamete and the oocyst wall (5).

Histology and immunocytochemistry. Portions of the small intestine or cecum (*E. tenella*) were removed and fixed in 2% paraformaldehyde in 0.1 M phosphate buffer, dehydrated, and embedded in wax. For histology, sections were stained with hematoxylin and eosin. For immunocytochemistry, sections were dewaxed and pressure cooked prior to immunolabeling. The sections were single labeled with anti-MORN1 or were double labeled with anti-TgMORN1 combined with one of the following: anti-TgENR, anti-TgIMC1, anti-TgENO2, anti-TgGRA7, anti-EtENR, anti-EmAPGA, or anti-EtAMA2. After tissue sections were washed, the location of the primary antibody was visualized by using either goat anti-rabbit immunoglobulin (Ig) conjugated to fluorescein isothiocyanate (FITC) for single labeling or a mixture of anti-rabbit Ig conjugated to FITC and goat anti-mouse Ig-conjugated Texas Red. After being washed, the sections were exposed to 4′,6′-diamindino-2-phenylindole (DAPI), washed, and mounted. Sections were examined by using a fluorescence microscope, and images were recorded by using Openlab software (Improvision).

Smears of sporozoites of *E. tenella* and *P. falciparum*-infected erythrocytes containing mature parasites were fixed in 2% paraformaldehyde and then acetone before being air dried. The smears of *P. falciparum* were pretreated by an antigen-retrieval method involving heat treatment (80°C) in citrate buffer prior to staining with anti-TgMORN1. After blocking with 1% bovine serum albumin (BSA)-phosphate-buffered saline (PBS), slides of both parasites were stained with anti-TgMORN1, washed, and visualized with goat anti-rabbit Ig conjugated to FITC. Slides were exposed to DAPI and mounted prior to examination.

Electron microscopy and immunoelectron microscopy. Small pieces of the surface mucosa of the small intestine or cecum were fixed in 4% glutaraldehyde in 0.1 M phosphate buffer for routine electron microscopy. For transmission electron microscopy, the samples were postfixed in osmium tetroxide, dehydrated in ethanol, treated with propylene oxide, and embedded in Spurr's epoxy resin. Sections were stained with uranyl acetate and lead citrate prior to examination with a JEOL 1200EX electron microscope (9). For scanning electron microscopy, small slices (through the mucosa) were dehydrated, critical point dried, mounted on stubs, sputter coated with gold, and examined under a Philips 505 scanning electron microscope.

For immunoelectron microscopy, small pieces of tissue were fixed in 2% paraformaldehyde in 0.1 M phosphate buffer, dehydrated, and embedded in LR White acrylic resin. Thin sections on Formvar-coated nickel grids were floated on drops of 1% BSA in PBS to block nonspecific staining, followed with the use of primary antibody, anti-TgMORN1. After being washed, sections were floated on drops of goat anti-rabbit Ig conjugated to 10-nm gold particles. The sections were stained with uranyl acetate prior to examination with the electron microscope (9).

***P. falciparum* cell fractionation.** Synchronous cultures of *P. falciparum* parasites were harvested at the ring stage (6 to 12 h), the trophozoite stage (18 to 24 h), and the schizont stage (36 to 42 h). Cells were solubilized in 150 mM NaCl, 5 mM EDTA, 50 mM Tris (pH 8.0), 1% Triton X-100 with protease inhibitors to generate the Triton X-100-soluble fraction. Triton X-100-insoluble pellets were then extracted in the same buffer supplemented with 2% sodium dodecyl sulfate (SDS) to produce the Triton X-100-insoluble, SDS-soluble fraction. Cocultured uninfected human red blood cells were processed as described above to provide control samples for subsequent analysis. The samples were subjected to SDS-polyacrylamide gel electrophoresis (10% acrylamide) and blotted onto nitrocellulose membranes. Immunodetection was carried out using ECL reagents (Amersham) with anti-TgMORN1 antibody (1:1,000 dilution) and peroxidase-conjugated swine anti-rabbit secondary antibody (1:1,000 dilution; DAKO).

***E. tenella*-stage isolation and Western blotting. (i) Sporozoites.** Sporozoites were recovered from cleaned oocysts by in vitro excystation and purified by anion exchange chromatography over columns of nylon wool and DE-52 cellulose (32).

(ii) In vitro first-generation schizogony. Monolayers of Madin-Darby bovine kidney cells (Flow Laboratories) were seeded into 24-well culture plates (Nunc) in Ham's F-12 nutrient medium with 10% fetal calf serum and infected with 250,000 freshly sporulated sporozoites. Cells were then cultured at 41°C in 5% CO_2 until first-generation schizonts were observed. Samples were taken at 40 h (mid-stage schizonts) and 55 h (late-stage schizonts) postinfection. The cell medium was aspirated, the monolayers were washed three times, the number of schizonts per well was counted, and cells were scraped into 100 μl PBS containing protease inhibitors.

(iii) In vivo second-generation merozoites. Second-generation merozoites were recovered from the cecal mucosa of chickens at 112 h after oral inoculation with 5×10^5 sporulated oocysts (36).

(iv) Gametocytes. Chickens at 4 weeks of age were infected with 10,000 oocysts. The chickens were killed at 143 to 145 h postinfection, and the ceca were removed and washed with cold SAC (170 mM NaCl, 10 mM Tris-HCl, pH 7, 10 mM glucose, 5 mM $CaCl_2$, 1 mM phenylmethanesulfonyl fluoride, 1 mg ml^{-1} BSA). The ceca were slit open and incubated at 37°C in a beaker with 0.5 mg ml^{-1} hyaluronidase in SAC (five ceca in 50 ml). The ceca were placed on top of a 17-μm mesh filter, and the mucosae were washed through with SAC (room temperature). The material left on the mesh was discarded, and the flowthrough was filtered through a 10-μm mesh filter. The gametocytes accumulated on this filter and were washed off with SAC and centrifuged at $800 \times g$ for 5 min (44).

The Western blot analysis was set up using standard procedures. Proteins from each sample were resolved by electrophoresis through 4 to 15% gradient SDS-polyacrylamide gel electrophoresis gels and transferred to nitrocellulose membranes by semidry blotting. Nonspecific binding sites were blocked by incubation for 1 h in 5% BSA in PBS, and then filters were probed with anti-MORN1, followed by goat anti-rabbit IgG conjugated to horseradish peroxidase. Binding was visualized by ECL (Amersham).

RESULTS

Asexual replication of *T. gondii* in the definite host by endopolygeny. The asexual development of *T. gondii* in the cat intestine has previously been described as involving a proliferative phase with repeated nuclear divisions, followed by a differentiation phase involving daughter formation. Daughter formation is initiated within the mother cell cytoplasm and progresses internally (Fig. 1 and 2A). Because more than two daughters are forming, this mechanism has been termed endopolygeny (11, 14, 30). The process was examined by double-labeled immunofluorescence using anti-TgMORN1 combined with anti-ENR, anti-ENO2, anti-GRA7, or anti-IMC1 to assist in identifying the individual developmental stages. It was observed that the early multinucleate stages, possessing elongate and branched ENR-positive apicoplasts, were unstained with MORN1 (data not shown). However, in the later stages, with multiple fragmented ENR-positive apicoplasts and ENO2-positive nuclei, there were multiple MORN1-positive ring-like structures distributed within the mother cell cytoplasm (Fig. 2C). To identify the subcellular location of MORN1, immunoelectron microscopy was employed. At an early stage in daughter formation, the eccentric nuclear spindle present in each of the multiple nuclei was labeled for MORN1 (Fig. 2B). In addition, the free ends of the cone-shaped structures formed by the daughter IMC were also labeled (Fig. 2B). The labeling appeared at the ends of the IMC as small clumps of gold particles in longitudinal sections (arrowheads, Fig. 2B) or an elongate line of gold particles in tangential sections (Fig. 2B). Two daughters formed in association with each nucleus and

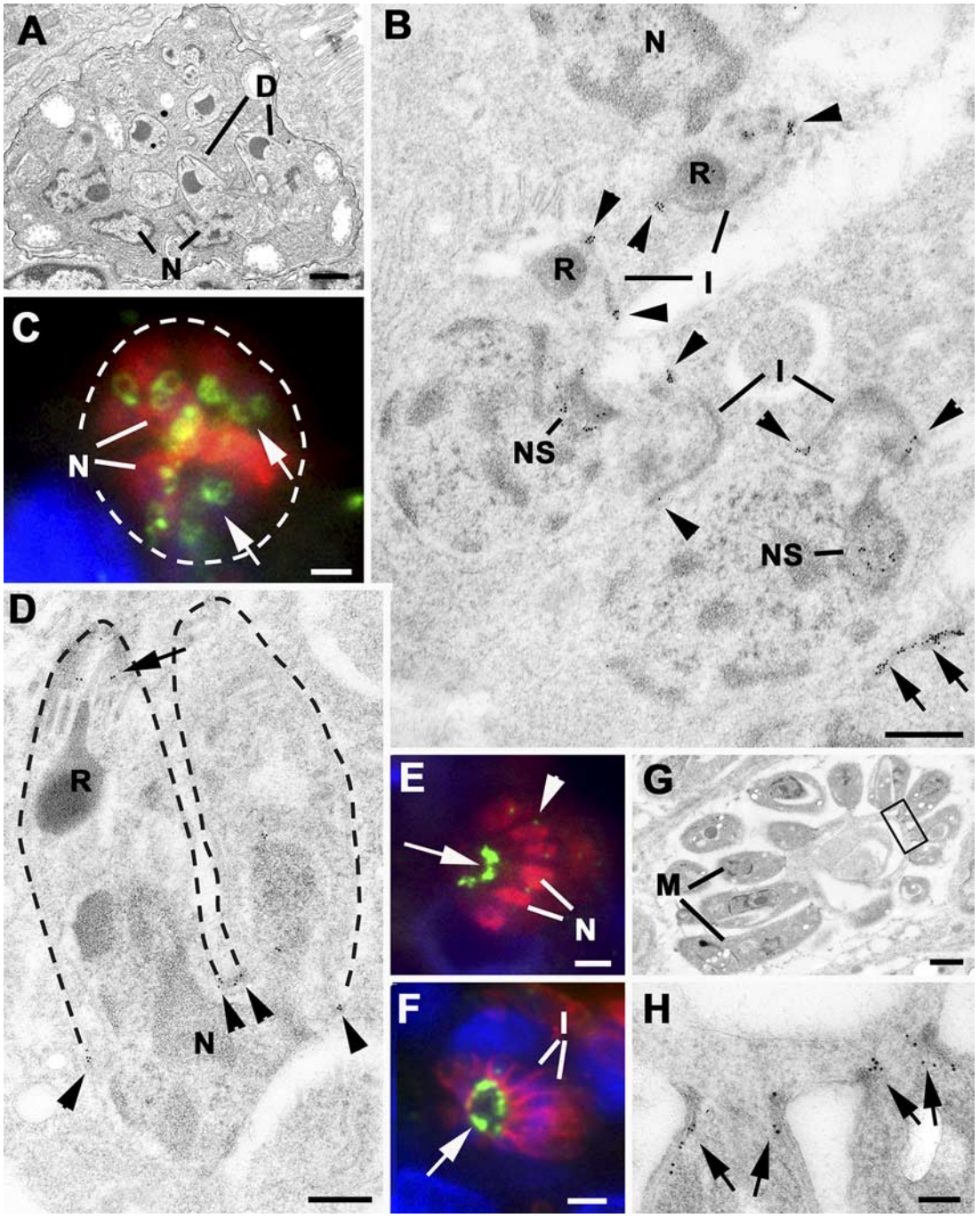

FIG. 2. MORN1 distribution during endopolygeny of *T. gondii* in the cat intestinal epithelium. (A) Transmission electron micrograph of a parasite in mid-stage *Toxoplasma* endopolygeny, showing the internally located cone-shaped IMCs of the developing daughters (D) associated with the multiple nuclei (N). Bar = 1 μm. (B) Electron micrograph of the early stage in daughter formation; immunostaining was done with TgMORN1 antibody, and labeling was done with 10-nm gold particles. Note the gold particles localizing to the spindle poles (NS) of the multiple nuclei (N) and the posterior extremities of the cup-shaped (arrowheads), newly forming, inner membrane cytoskeleton scaffolds (I). In addition, one IMC has been cut tangentially through the base of the cone, showing gold particles along its length (parallel arrows in the lower right corner). Bar = 100 nm. (C) Fluorescent micrograph of *T. gondii* (in a stage of endopolygeny similar to that shown in panel A) double labeled with anti-MORN1 (green) and ENO2 (red) counterstained with DAPI (blue). A number of MORN1-positive rings (arrows), often in pairs (arrows), are observed over the ENO2- and DAPI-positive nuclei (N) distributed throughout the cytoplasm. Bar = 1 μm. (D) Detail of part of an immunoelectron micrograph of a schizont showing more advanced daughter formation with the IMCs (outlined by the dotted lines) enclosing the ends of the crescent-shaped nucleus (N). Arrowheads mark MORN1-specific gold particles at the sites of posterior budding of the IMC. In addition, apical staining is observed (arrow). R, rhoptry. Bar = 100 nm. (E) Immunofluorescence section stained with anti-MORN1 (green) and ENO2 (red) showing a mature schizont with fully formed merozoites. Note the strong MORN1 staining of the basal end of the merozoites (arrow), with weak labeling of the nuclear pole (arrowhead). N, nucleus. Bar = 1 μm. (F) Immunofluorescence section stained with anti-MORN1 (green) and anti-IMC (red), showing a mature schizont with fully formed merozoites. The merozoites are outlined in red due to the IMC staining and exhibit strong posterior staining for MORN1 (arrow). I, IMC. Bar = 1 μm. (G) Immunoelectron micrograph of a mature schizont labeled with anti-MORN1, showing the fully formed merozoites (M) still connected by their posterior ends to the residual cytoplasmic mass. Bar = 1 μm. (H) Enlargement of the enclosed area in panel G showing numerous gold particles associated with the basal end of the IMC (arrows). Bar = 100 nm.

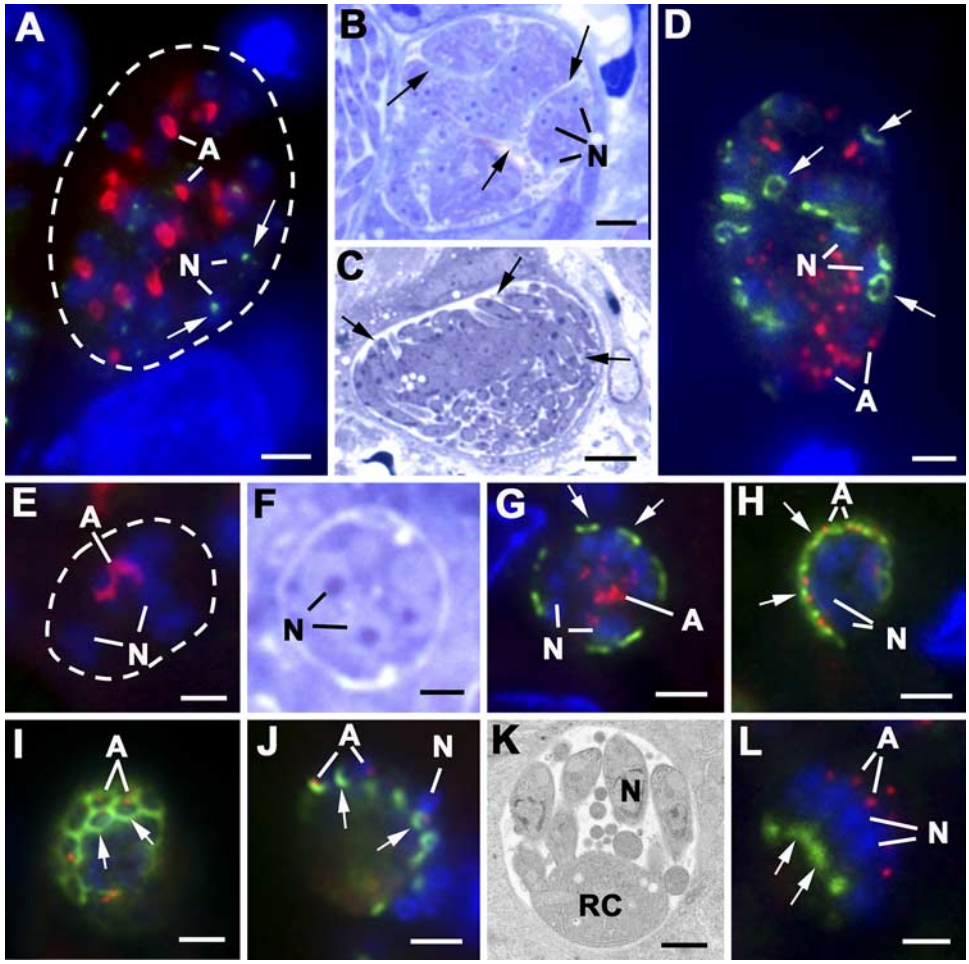

FIG. 3. Schizogony in *E. tenella* (A to D) and *E. acervulina* (E to L) in sections of chicken gut was examined by immunofluorescence (A, D, E, G to J, and L), light microscopy (B, C, and F), and electron microscopy (K). The immunofluorescent sections were labeled with anti-MORN1 (green) and anti-ENR (red) that identifies the apicoplast and counterstained with DAPI (blue). (A) Fluorescence micrograph of a large mid-stage schizont showing the multiple nuclei (N) and a number of large ENR-positive apicoplasts (A). The only MORN1 staining observed was that of a single small relatively weak staining structure toward the periphery of the nuclei (arrows). Dotted line outlines parasite. Bar = 1 μm. (B and C) Light micrographs of 1-μm plastic sections illustrating large multinucleated schizonts. (B) Stage prior to the initiation of daughter formation showing the nuclei (N) close to the plasmalemma and its deep invaginations (arrows). (C) Later stage showing the early formation of daughters at the surface of the schizont (arrows). Bars = 5 μm. (D) Schizont at an early stage of daughter formation identified by the presence of MORN1-positive material at the plasmalemma and its invaginations, which in certain orientations has a ring-like appearance (arrows). Note the numerous nuclei (N) and the fragmented apicoplast (A). Bar = 1 μm. (E) Small schizont (outlined by dotted line) with relatively few nuclei (N) and a single elongate ENR-positive apicoplast (A). Note the absence of any MORN1 staining at this stage. Bar = 1 μm. (F) Light micrograph of a stage similar to that shown in panel E, illustrating the few nuclei (N) contained within the schizont. Bar = 1 μm. (G) Schizont with peripherally located nuclei (N) and a fragmented centrally located apicoplast (A). A number of MORN1-positive plaques located at the plasmalemma directly above the nuclei represent the initiation of daughter formation (arrows). Bar = 1 μm. (H) Stage (slightly later than that shown in panel G) in which the individual apicoplasts (A) have relocated adjacent to the nuclei (N) close to the peripherally located MORN1-positive plaques (arrows). Bar = 1 μm. (I) Tangential section through the surface of a schizont at a stage (similar to that shown in panel H) showing the tightly packed MORN1-positive rings associated with early daughter formation (arrows). Bar = 1 μm. (J) Later stage in daughter formation, showing the MORN1-positive rings representing that the posterior growth of the IMC has advanced beyond the apicoplasts (A) and nuclei (N). (K) Electron micrograph of a late schizont showing the daughters still connected to the residual cytoplasm (RC). N, nucleus. Bar = 1 μm. (L) Late-stage schizont in which the fully formed daughters possess nuclei (N) with associated apicoplasts (A) and show strong MORN1-positive staining of their posterior end (arrow). Bar = 1 μm.

were located above the nuclear poles (Fig. 2B and C). As the posterior growth of the IMC continued, they started to enclose various organelles, with each nucleus dividing between two daughters (Fig. 2D). During this process, the ends of the IMC remained labeled with MORN1 and there was evidence of low-level labeling of the anterior ring of the IMC (Fig. 2D). This growth continued until the daughters were fully formed and occupied all the space within the mother cell (data not shown). The final stage involved invagination of the mother cell plasmalemma around each of the daughters from anterior to posterior to form the characteristic pellicle with the posterior of each daughter remaining attached to a small amount of residual cytoplasm (Fig. 2E to H). The posterior ring formed by the IMC was still strongly labeled for MORN1 (Fig. 2E to G).

MORN1 in classical *Eimeria* species schizogony. In a manner similar to that for *Toxoplasma* endopolygeny, schizogony also involves a proliferative phase with repeated nuclear divisions, followed by a differentiation phase involving daughter formation by budding from the mother cell surface (Fig. 1E and F). The number of daughters produced varies significantly between species and even between asexual generations within each species. The number of daughters ranges from approximately 16 (*E. acervulina* and *E. maxima*) to many hundreds (*E. tenella*). When schizonts produce large numbers of daughters, the surface area is increased by multiple deep invaginations of the plasmalemma (Fig. 3B) (14).

In *E. tenella*, a large number of nuclear divisions gives rise to over 100 nuclei (Fig. 3B) and a number of large apicoplasts (Fig. 3A). In *E. acervulina*, there are fewer nuclear divisions, giving rise to approximately eight nuclei (Fig. 3F) with a single elongated apicoplast (Fig. 3E). In both cases, the schizonts did not stain with anti-MORN1, although in certain samples, light staining of the nuclear pole was visible (Fig. 3A). At the end of the proliferative phase, the nuclei move to the periphery of the mother cell and locate beneath the plasmalemma (Fig. 3C and F). The first evidence of daughter formation was the appearance of MORN1-positive plaques beneath the mother cell plasmalemma (Fig. 3G) or its invaginations in *E. tenella* (Fig. 3D). The initiation of daughter formation coincides with fragmentation of the apicoplast (Fig. 3D and G). By electron microscopy, the plaques appear to represent the IMC of each of the developing daughters and possess a centrally located conoid (Fig. 4A) and underlying microtubules (Fig. 4C). Each IMC was located beneath the plasmalemma, directly above a nuclear pole/centriolar complex (Fig. 4A). The two nuclear pole/centriolar complexes formed during the final division of each nucleus were each directed toward a developing daughter (Fig. 4C). By immunoelectron microscopy staining for MORN1, it was possible to identify gold particles at the free ends of the IMC at the point where the daughters are budding into the parasitophorous vacuole (Fig. 4B and E). As the daughters form by growth at the posterior end of the IMC, the growing edge remains in close contact with the plasmalemma, resulting in the daughters appearing to bud out from the surface (Fig. 3C and 4C and D). The progressive formation of the daughters can be difficult to illustrate in the large schizonts of *E. tenella* due to the size and complexity of daughter formation (Fig. 3C and 4D). However, in the small schizonts of *E. acervulina*, it was easier to follow the morphological changes. It was observed that after fragmentation of the apicoplast (Fig. 3G), the individual small apicoplast reoriented to become associated with the nuclei located beneath the MORN1-positive plaques (Fig. 3H). In more tangential sections, the plaques appeared as closely packed, ring-like structures (Fig. 3I). As the daughters grow, the MORN1-positive rings appear to move over the nuclei (Fig. 3J) and end with strongly positive posterior staining, where the daughters remain connected to the residual cytoplasm (Fig. 3K and L). This strong labeling of the posterior ring was also confirmed in the late stages of merozoite formation in *E. tenella* by electron microscopy (Fig. 4F and G). However, with detachment and release of the mature merozoites, it appeared that the strong posterior staining was greatly reduced, although the nuclear pole was still stained (data not shown).

To confirm the expression of MORN1, attempts were made to isolate various parasite stages of *E. tenella*. It was possible to obtain pure samples of sporozoites, which showed anti-TgMORN1 staining of the posterior ring, the nuclear pole and weak staining of the anterior ring (Fig. 4H and I) in a manner similar to that reported for the *T. gondii* tachyzoite (15). In Western blots, this sample showed a single band of approximately 41 kDa (Fig. 4J, lane 1). In the relatively pure samples obtained from the in vitro-cultured first-generation schizonts, similar bands were identified in the mid-stage (Fig. 4J, lane 2) and late-stage (Fig. 4J, lane 3) schizonts compared to the uninfected culture cells that were negative (Fig. 4J, lane 6). Unfortunately, no band was observed for the in vivo-produced merozoites (Fig. 4J, lane 4), although a very weak band was observed for the gametocyte fraction (Fig. 4J, lane 5).

MORN1 localizes to the merozoite budding sites on *Plasmodium* schizonts. To consolidate the case for a conserved role of MORN1 across the different modes of zoite budding, schizogony of *P. falciparum* in the red blood cell was examined. Due to the small size of *P. falciparum* and the ability to culture in vitro, no sectioning is required, which allows the entire schizont and developing merozoites to be examined. Initially, the multinucleate stages were unstained with anti-MORN1, but in the later stages, a number of MORN1-positive plaques or rings (depending on the orientation) were observed on the surface (Fig. 5A to C). It was possible to identify 16 rings in the majority of schizonts (Fig. 5A to C). Posterior growth of the rings appears to result in the formation of 16 merozoites with strong posterior staining in addition to an anterior MORN1-positive structure probably representing the nuclear pole (Fig. 5D to F), but this will require further confirmation. Therefore, the distribution of MORN1 during schizogony in *P. falciparum* was identical to that observed for *Eimeria* species.

PfMORN1 is expressed late in schizogony and fractionates into both detergent-soluble and -insoluble fractions. MORN1 in *T. gondii* tachyzoites fractionates into detergent-soluble and -insoluble fractions, indicating that MORN1 is in part associated with the cytoskeleton and likely forms a bridge to the membrane component of the IMC (15). Since MORN1 localization across division modes was reminiscent of dividing tachyzoites, we sought to perform similar extraction for other parasites and division modes. It was not possible to obtain sufficiently pure samples from the chicken gut to carry out Western blotting studies of the MORN1 associated with development in *Eimeria* species. However, in the in vitro-cultured *P. falciparum*, it was possible to obtain parasites at various stages throughout their intraerythrocytic development and to extract the cells with 1% Triton X-100 (Fig. 5G). Western blotting with the anti-TgMORN1 antibody identified a single band of the expected size (41.4 kDa) for PfMORN1 (Fig. 5G). Furthermore, the Western blot showed that PfMORN1 was absent or under the level of detection in the early stages of development (ring and trophozoite), but it was easily detectable in later stages (38 to 48 h), which coincides with the late stages in schizogony and merozoite budding. As observed previously by Gubbels et al. for *T. gondii* tachyzoites (15), the *Plasmodium* blot showed that MORN1 was found in both detergent-soluble and -insoluble fractions (Fig. 5G).

MORN1 distribution during sexual development within the Coccidia. Sexual development of Coccidia takes place in the

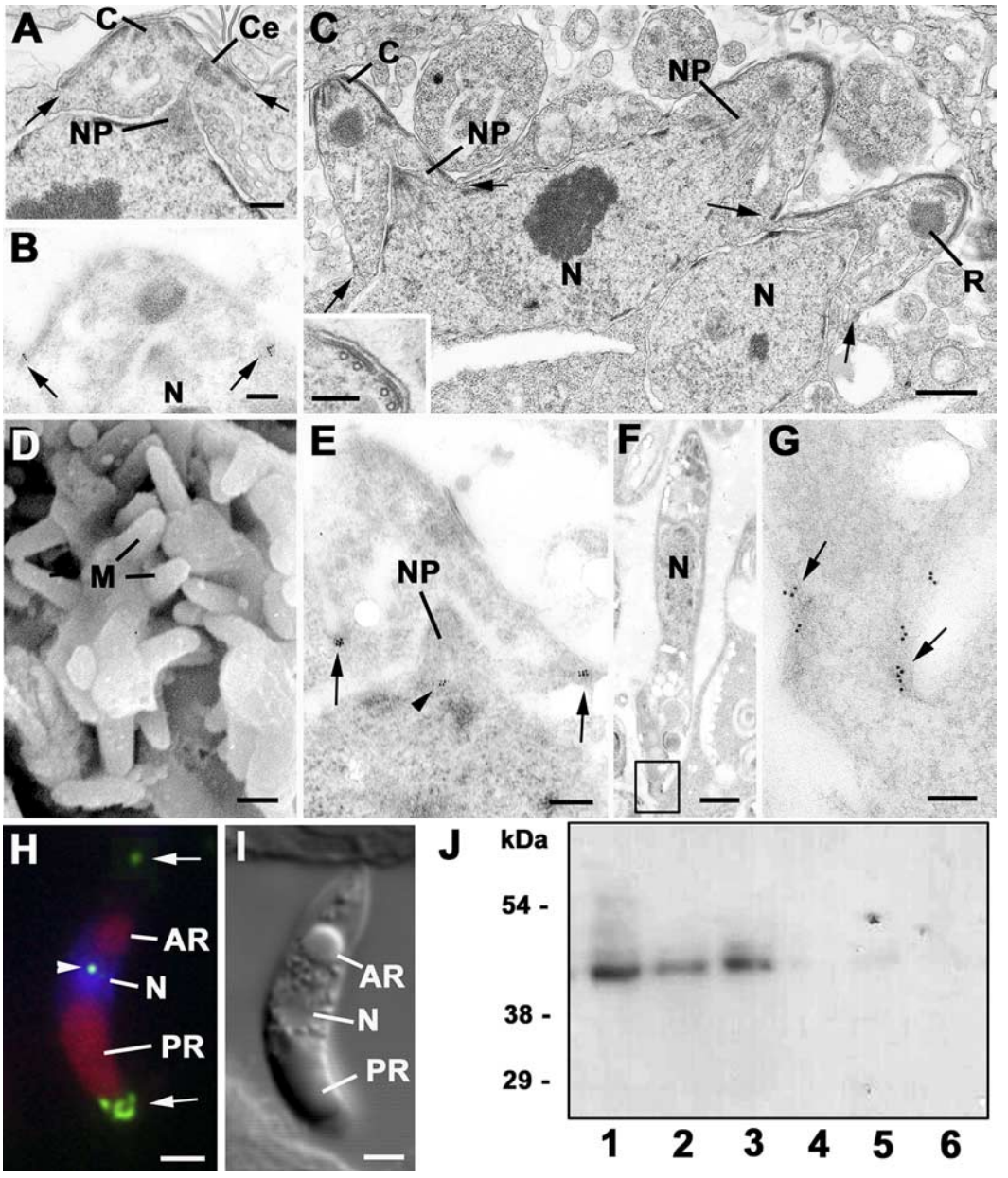

FIG. 4. Electron micrographs of sections routinely processed (A and C) and sections immunostained with anti-MORN1 (B, E, F, and G) plus a scanning electron micrograph (D) of schizogony of *E. tenella* in chicken cecum. (A) Detail of part of the surface of a mid-stage schizont, illustrating the early stage in daughter formation, with cone-shaped dense IMC with central conoid (C) close to the plasmalemma (arrows) and directly above a nucleus with the nuclear pole (NP) and centrioles (Ce) directed toward the IMC. Bar = 100 nm. (B) Developmental stage (similar to that shown in panel A) immunostained for MORN1 showing the gold particles located at the free ends of the IMC (arrows). N, nucleus. Bar = 100 nm. (C) Part of the surface at a slightly later stage, showing three daughters budding out into the parasitophorous vacuole. In the upper nucleus (N), the two nuclear poles (NP) can be seen directed toward developing daughters. Note that the IMC is associated with the budding daughters, with the free end located at the junction with the plasmalemma of the mother cell (arrows). R, rhoptry. Bar = 500 nm. (Insert) Detail of part of a cross section through a developing daughter, showing the inner membrane plaques with underlying microtubules adjacent to the plasmalemma forming the intact pellicle. Bar = 100 nm. (D) Scanning electron micrograph of part of a schizont showing the irregular surface invaginations and the irregular orientation of the numerous merozoites budding from the surface (M). Bar = 1 μm. (E) Immunostained section of a stage similar to that shown in panel C showing clumps of gold particles associated with the free end of the IMC (arrows). Note the lightly labeled (arrowhead) nuclear pole (NP) directed toward the interior of the developing daughter. Bar = 100 nm. (F) Low-power magnification of part of a late-stage schizont, illustrating a fully formed merozoite still attached to the residual cytoplasm (enclosed area). N, nucleus. Bar = 1 μm. (G) Enlargement of the enclosed area in panel F, showing numerous gold particles associated with the basal end of the IMC (arrows). Bar = 100 nm. (H and I) Immunostained (H) and phase-contrast (I) images of a sporozoite of *E. tenella* showing the nucleus stained with DAPI (N) and the anterior (AR) and posterior (PR) refractile bodies, which autofluoresce slightly red. Note the anti-MORN1 staining associated with the anterior and posterior rings (arrows) and the nuclear pole (arrowhead). Bar = 1 μm. (J) Western blot in which lane 1 shows the sporozoite sample, lane 2 shows the in vitro-cultured, mid-stage, first-generation schizonts (40 h postinfection), lane 3 shows the late-stage, first-generation schizonts (55 h postinfection), lane 4 shows the in vivo second-generation schizonts (112 h postinfection), lane 5 shows the in vivo gametocyte sample (148 h postinfection), and lane 6 shows uninfected MDCK cells. The membranes were probed with anti-TgMORN1 as a first layer and peroxidase-conjugated swine anti-rabbit secondary antibody. Note the single band present in the sporozoite and the mid-stage and late-stage in vitro schizonts and a weak staining band in the gametocyte sample, all at approximately 41 kDa.

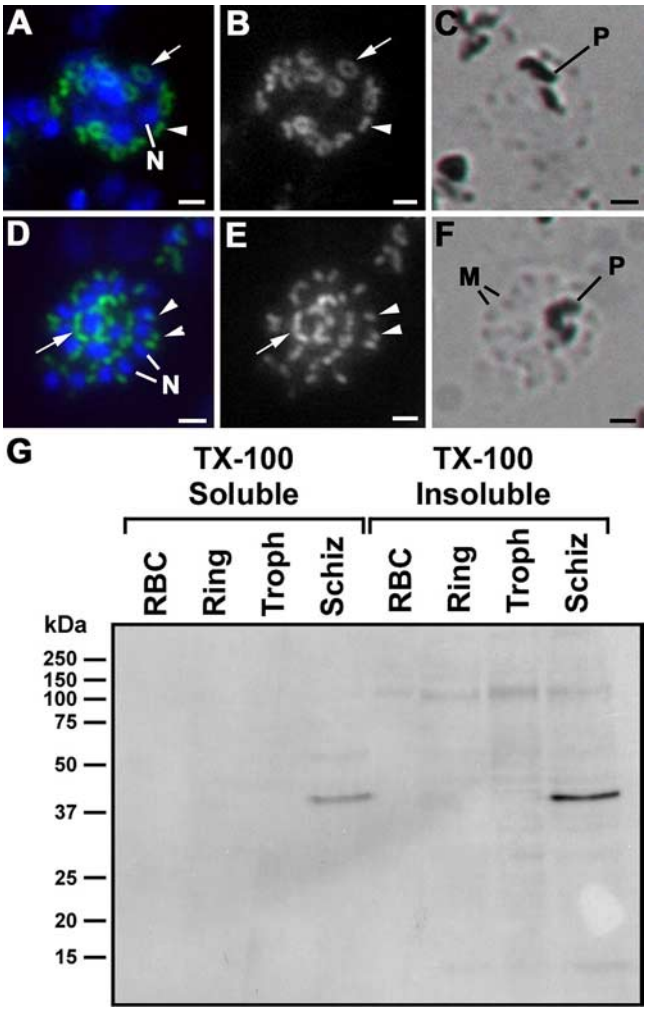

FIG. 5. MORN1 in schizogony of *Plasmodium*. Images of infected erythrocytes immunostained with anti-MORN1 (green) and the nuclei counterstain showing the DAPI-positive nucleus (blue) (A and D). Panels B and E present the green channel in gray, increasing the clarity of the MORN1-positive staining. Panels C and F represent the transmitted light image. (A to C) Infected erythrocyte illustrating a late stage in schizogony in which 16 individual MORN1-positive rings (tangential appearance [arrows]) or plaques (longitudinal orientation [arrowheads]), representing the free ends of the cone-shaped IMCs, can be identified. (D to F) Infected erythrocyte containing a mature schizont showing the DAPI staining of nuclei (N) of the daughters with strong posterior MORN1 staining (arrows) and a smaller, more apical MORN1-positive structure, possibly representing the nuclear pole (arrowheads). The transmitted light images illustrate the dark-appearing hemozoin pigment (P) in panels C and F. In panel F, individual merozoites (M) can be identified. Bars = 1 μm. (G) Western blot of the Triton X-100-soluble and Triton X-100-insoluble fractions from uninfected erythrocytes and erythrocytes infected with *P. falciparum* at various stages of development. A single band was identified in the Triton X-100-soluble and Triton X-100-insoluble fractions of schizont-stage parasites, and it was of a molecular weight matching the expected size (41 kDa) of PfMORN1. RBC, red blood cells; Troph, trophozoite; Schiz, schizont.

cecum and small intestine, resulting in microgametes and macrogametes with morphological features reminiscent of male and female gametes, respectively. Microgametogony gives rise to a variable number of motile microgametes, whereas macrogametogony gives rise to a single macrogamete. Sexual development was studied across four coccidian species: *T. gondii*, *E acervulina*, *E. tenella*, and *E. maxima*. They developed in similar manners and varied only in size and the number of gametes formed. Therefore, coccidian sexual development will be represented in a combined description without differentiating between the species. Various stages in the development of the two processes were observed located in adjacent epithelial cells (Fig. 6A, B, and D and 7A).

During macrogametogony, the invading merozoite grows into a large spherical structure with a single large electron lucent (determined by transmission electron microscopy) and DAPI-negative nucleus (determined by immunofluorescence) (Fig. 6B to E). Maturation involved the synthesis of numerous polysaccharide granules and lipid droplets in addition to a number of large granules termed wall-forming bodies (Fig. 6A, B, and D and 7A). When examined for MORN1 expression, no positive material was observed (Fig. 6C and E).

In microgametogony, as the invading merozoite grows, it loses its IMC confirmed by the absence of staining with anti-IMC1 (data not shown) and undergoes a variable number of nuclear divisions. During this proliferative phase, it is not possible to differentiate between parasites that will undergo asexual development and those that will form microgametes. In all four species, the nuclei move to the periphery of the mother cell (Fig. 6F and G and 7A) or invaginations of the plasmalemma in the large microgametocytes of *E. maxima* (Fig. 6B and C). Only the single nuclear pole in each nucleus was labeled with anti-MORN1 and was always directed toward the plasmalemma (Fig. 6F and 7B). This stage was followed by the appearance of MORN1-positive plaques directly above the nuclear pole and adjacent to the plasmalemma (Fig. 6H and J). In tangential sections, the plaques appear as rings of MORN1-positive material (Fig. 6I) and, in certain cases, the rings had a targetoid appearance due to the central MORN1-positive nuclear pole (Fig. 6I). By electron microscopy, two small clumps of gold particles were observed adjacent to the plasmalemma, consistent with cross sections through the MORN1-positive ring (Fig. 7C). This observation was followed by condensation of the heterochromatin within each nucleus into a single clump at the side adjacent to the centrioles and plasmalemma (Fig. 7A). This result coincides with a loss of the MORN1-positive nuclear pole, but was associated with a marked increase in the MORN1 signal (Fig. 6C and H to J). At this point, the centrioles appear to convert to two basal bodies from which flagella start to grow, protruding into the parasitophorous vacuole enclosed by the mother cell plasmalemma (Fig. 7D). Microgamete formation was initiated by the protrusion of cytoplasm containing the basal bodies, a dense portion of the nucleus, and a mitochondrion passing through the ring formed by the collar of electron-dense material beneath the plasmalemma (Fig. 7E). As this proceeds, the electron-dense portion of the nucleus separates from the electron lucent portion, which remains in the mother cell as a residual nucleus. During this movement, the electron-dense collar was MORN1 positive (Fig. 7G), but gold particles were also observed in the immature microgamete cytoplasm adjacent to the mitochondrion (Fig. 7G). By light microscopy, the microgamete nuclei appeared as small, spherical, dense structures at the periphery of the microgametocyte (Fig. 6K). By immunofluorescence, the

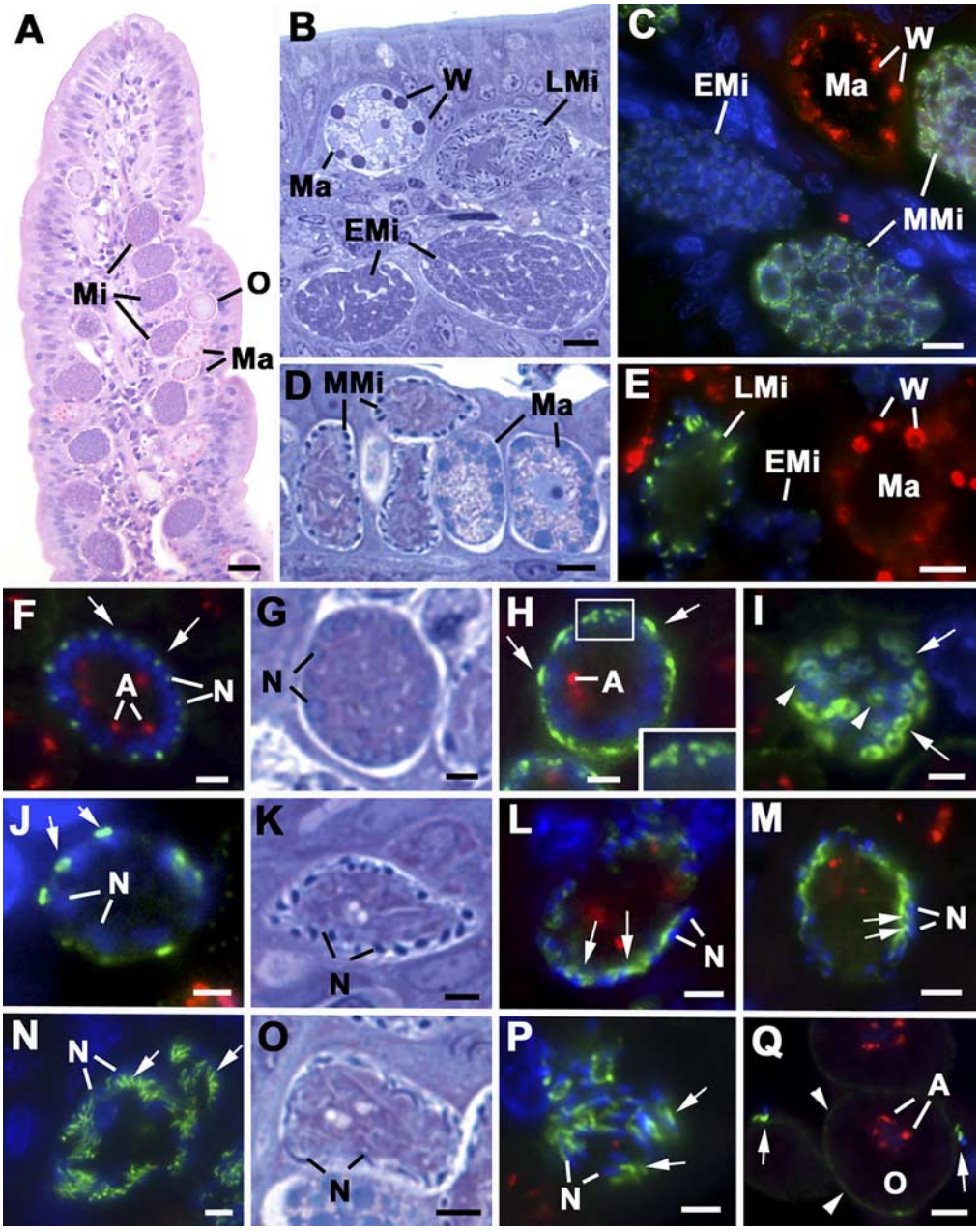

FIG. 6. Sections illustrating the light microscopic (A, B, D, G, K, and O) and immunolight microscopic (C, E, F, H to J, L to N, P, and Q) appearances of the sexual development of various coccidian parasites in the intestine of the definitive host. The immunostained sections were labeled with anti-MORN1 (green) combined with anti-APGP (wall-forming bodies stained red) (C and E) or anti-ENR (apicoplasts stained red) (F, H to J, L to N, P, and Q), and all were counterstained with DAPI (blue). The light microscopy for morphology consisted of wax sections stained with hematoxylin and eosin (A) or 1-μm plastic sections stained with Azure A (B, C, G, K, and O). (A) Low-power magnification of a longitudinal section through a villus of a chicken infected with *E. maxima*, illustrating numerous developmental stages of microgametocytes (Mi) and macrogametocytes (Ma) and early oocyst formation (O) within the epithelial cells. Bar = 10 μm. (B and D) Moderate-power magnification showing sexual development of *E. maxima* and *E. tenella*, respectively, showing early-stage (EMi), mid-stage (MMi), and late-stage (LMi) microgametocytes and an adjacent macrogametocyte (Ma) in panel B characterized by the presence of densely staining granules representing the wall-forming bodies (W). Bar = 5 μm. Panels C and E show sections containing sexual stages similar to those in panels B and D, respectively, in which the microgametocytes were labeled with anti-MORN1 (green), while the macrogametocytes (Ma) identified by the wall-forming bodies (W) were unstained. Note that in the early microgametocyte (EMi), there was low-intensity staining limited to the nuclear poles, while there was increased staining intensity in the mid-stage microgametocytes (MMi) and late microgametocytes (LMi) associated with microgamete formation. Bar = 5 μm. (F) Early microgametocyte of *E. tenella* showing the peripherally located nuclei (N), each with a single MORN1-positive spot on the outer aspect of each nucleus (arrows), while the cytoplasm contains a few small apicoplasts (A). Bar = 1 μm. (G) Light microscopy (of a stage similar to that shown in panel F) showing the peripherally located nuclei (N). Bar = 1 μm. (H) Early microgametocyte of *E. acervulina* in which MORN1-positive plaques were present at the surface of the parasite (arrows) directly above each nucleus (N), representing the initiation of microgamete formation. A, apicoplast. Bar = 1 μm. (Insert) Enlargement of the enclosed area in panel H in which it was possible to resolve the MORN1-positive nuclear pole just beneath the MORN1-positive plaque. Bar = 500 nm. (I) Tangential section through the surface of an *E. acervulina* microgametocyte (similar to that shown in panel H) illustrating the ring-like appearance of the plaques in cross section (arrows). A few have targetoid appearances, where the centrally located MORN1-positive nuclear pole was also visible (arrowhead). Bar = 1 μm. (J) Early microgametocyte of *T. gondii* showing relatively few MORN1-positive plaques (arrows) at the surface above the nuclei (N). Bar = 1 μm. (K) Light

nuclei were strongly stained with DAPI and had moved from being internal to the MORN1-positive material (Fig. 6H to J) to being located on the external side of the MORN1-positive rings (Fig. 6L and M). The microgamete matures while still attached by its anterior to the mother cell by an aperture delineated by the electron-dense collar (Fig. 7F), which labels with MORN1 (Fig. 7H). Maturation involves the continued growth of the two flagella and elongation of the mitochondrion, which is located close to the basal bodies and partially overlaps with the DAPI-positive, elongated, crescent-shaped nucleus (Fig. 6N and O and 7F and H). This was also associated with an elongated appearance of MORN1 staining material in the anterior of the microgamete (Fig. 6M, N, and P), which correlated to the numerous gold particles observed in the microgamete anterior around the mitochondrion (Fig. 7K, L, and M). The mature microgamete is released by detachment from the ring-like collar. The anterior of each microgamete possesses two basal bodies from which long flagella protrude, an electron-dense, bar-like structure termed the perforatorium and four microtubules that run posteriorly over the mitochondrion and part of the nucleus (Fig. 6P and 7I and J). The free microgametes retain the strong anterior MORN1 staining, allowing individual microgametes to be identified by immunofluorescence within the gut lumen and close to early oocysts (Fig. 6Q). Immunoelectron microscopy showed a few gold particles at the apex (Fig. 7M), but the largest numbers were located in the cytoplasm between the mitochondrion and the plasmalemma (Fig. 7K, L, and M).

DISCUSSION

This study provides evidence that the antibody to TgMORN1 recognizes and stains the MORN1 homologues with the correct predicted molecular weight in *E. tenella* (Fig. 4J) and *P. falciparum* (Fig. 5G). From examination of the asexual and sexual processes, we observed that MORN1 has similar dynamic expression and localization patterns and therefore probably has a conserved function in the various members of the Apicomplexa. MORN1 has been identified at four distinct locations, the nuclear poles, the edges of the IMC during asexual development (the leading edge during formation is specifically enriched in MORN1), the site of budding of the microgamete, and the anterior of microgamete.

Nuclear localization. The early stages of *Toxoplasma* endopolygeny, schizogony, and microgametogony are indistinguishable and involve repeated nuclear division, giving rise to a multinucleate organism. At this stage, MORN1 staining was observed to be limited to the nuclear poles. This observation was described in detail during endodyogeny in *T. gondii*, where it was shown that MORN1 was associated with the characteristic conical-shaped structure of the nuclear pole, the centrocone, formed by a dilation of the nuclear membranes, which remain intact during division (15). In the present study, this location was confirmed across the Apicomplexa species examined. The presence and specific orientation of the MORN1-positive nuclear spindle pole and associated centrioles appear to act as an organizing unit for both daughter and microgamete formation. In both situations, this control mechanism will ensure that a nucleus will be associated with each developing zoite or microgamete, thus ensuring their viability. However, microgametogony is characterized by peripheral condensation of the nuclear chromatin and with loss of the nuclear pole, which is the first distinguishing morphological feature of microgametogony (11). In contrast, the zoites formed by all forms of asexual development retain the MORN1-positive nuclear pole throughout their transmission cycle, which is consistent with the case described previously for the tachyzoite of *T. gondii* (15).

Maintenance of MORN1 in the centrocone throughout the asexual cycle was also shown in the endopolygeny of *Sarcocystis neurona*, since here the polyploid nucleus has to be resolved into haploid zoites. The maintenance of the spindle and association with the chromosomes throughout the cell cycle ensures that each zoite is endowed with a single complete set of chromosomes (15, 43). However, the stability of MORN1 localization in the centrocone is not dependent on the presence of microtubules, as its localization remained unchanged upon incubation with the microtubule depolymerizing agent oryzalin (15). Therefore, it appears that in addition to the proposed involvement of MORN1 with nucleation of daughter scaffolds, it is likely also part of the structural complex organizing the spindle pole, where the microtubules penetrate the nuclear envelope. Both functions appear to be conserved throughout the different asexual division modes across the Apicomplexa.

Asexual replication. While there are distinct morphological differences in the various asexual processes undergone by apicomplexan parasites concerning the number and timing of nuclear divisions and the number and location of daughter formation (Fig. 1), the mechanism of daughter formation appears to have retained many similarities across the phylum. In all four processes, the formation of the IMC of the daughter pellicle appeared to be coordinated via the nuclear pole/cen-

micrograph of a mid-stage microgametocyte of *E. tenella* in which the dense staining spherical-shaped nuclei (N) are arranged around the periphery of the parasite. Bar = 1 μm. (L) Stage (similar to that shown in panel K) showing the spherical DAPI staining nuclei (N) now located on the external side of the MORN1-positive plaques (arrows). Bar = 1 μm. (M) Slightly later stage than that shown in panel L, showing that the nuclei (N) have started to elongate and an elongated MORN1-positive structure is present anterior to the nuclei (arrows). Bar = 1 μm. (N) Part of a late microgametocyte of *E. maxima* in which a large number of microgametes with crescent-shaped DAPI-positive nuclei (N) and elongated anterior MORN1-positive structures (arrows) are still attached to the mother cell. Bar = 1 μm. (O) Light micrograph of a late microgametocyte of *E. tenella* in which a number of mature microgametes with elongated nuclei (N) can be identified. Bar = 1 μm. (P) Late microgametocyte of *E. acervulina* showing a number of mature microgametes each with the DAPI-positive nuclei (N) and the elongated anterior MORN1-positive structure (arrows). Bar = 1 μm. (Q) Section through the lumen of a cecal crypt of a chicken infected with *E. tenella* in which two microgametes can be identified by the DAPI-positive nucleus and the undulating MORN1-positive anterior staining (arrows). Note that one is adjacent to an early oocyst (O) recognized by the slight autofluorescence of the oocyst wall (arrowheads) and the apicoplast (A) associated with the nucleus. Bar = 1 μm.

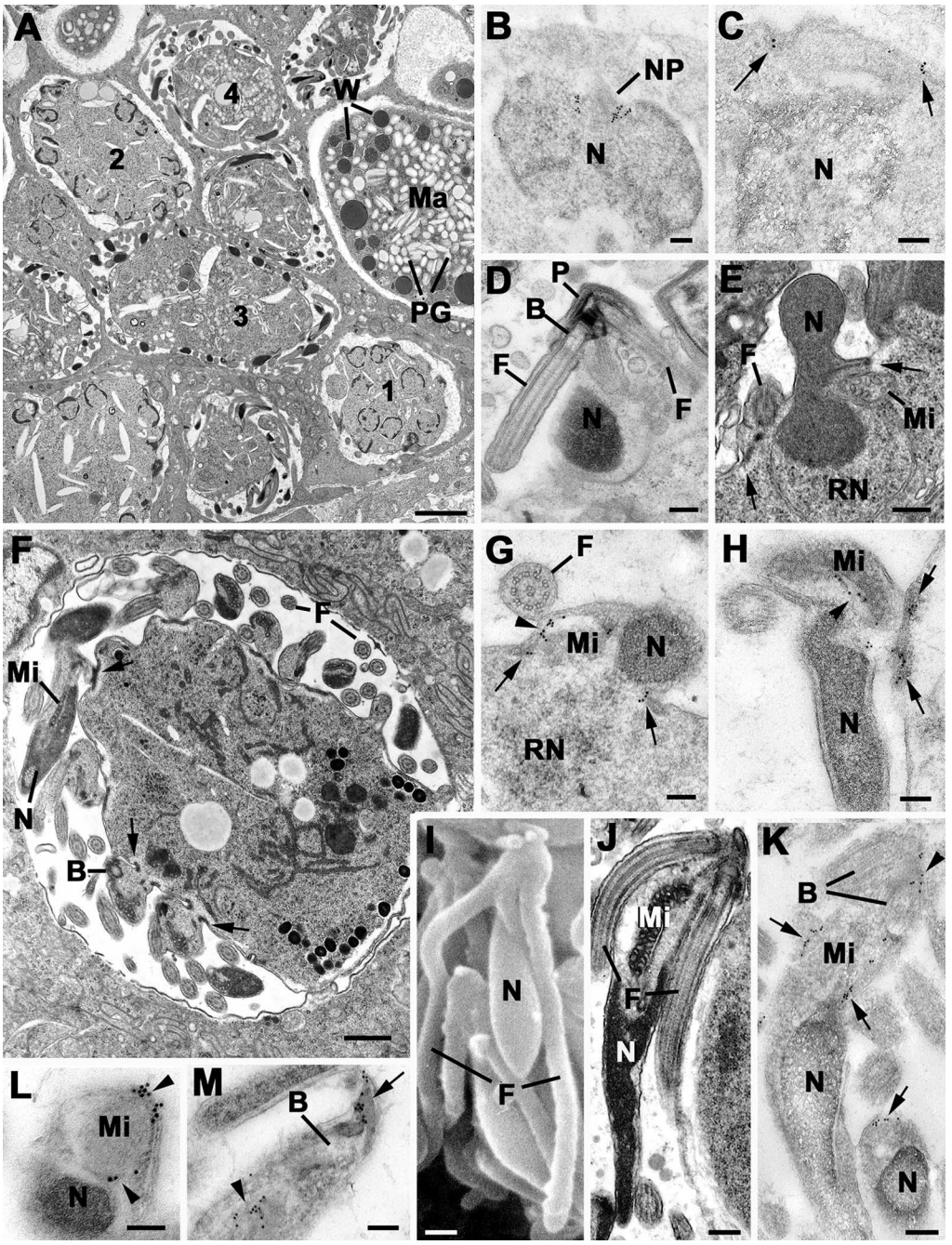

FIG. 7. Micrographs of microgametogony of coccidian parasites using routine transmission electron microscopy (A, D, E, F, and J), immunoelectron microscopy of sections stained with anti-MORN1 (B, C, G, H, and K to M), and scanning electron microscopy (I). (A) Micrograph (with low-power magnification) of an *E. tenella* infection showing part of a macrogametocyte (Ma) characterized by electron-dense granules representing the wall-forming bodies (W) and numerous polysaccharide granules (PG) plus a number of microgametocytes at various stages of maturity. Based on nuclear morphology, these range from the early stage (1) with open nuclei through the slightly later stage (2) with peripheral condensation of the chromatin to the middle stage (3), where the electron-dense mass of the nucleus has protruded into the parasitophorous vacuole, and finally the mature stage (4) with fully formed microgametes with elongate electron-dense nuclei located in the parasitophorous vacuole. Bar = 2 μm. (B) Part of the periphery of an early microgametocyte showing a nucleus (N) with a nuclear pole (NP) labeled with gold particles directed toward the plasmalemma. Bar = 100 nm. (C) Stage (similar to that shown in panel B) in which two clumps of gold particles (arrows) are located at the plasmalemma on either side of the nucleus (N). Bar = 100 nm. (D) Early stage in microgamete formation showing flagella (F) arising from the basal bodies (B) and growing into the parasitophorous vacuole. An electron-dense plaque at the anterior that represents the perforatorium (P) is also present. N, nucleus. Bar = 200 nm. (E) Detail in which the electron-dense portion of the nucleus (N) is protruding into the parasitophorous vacuole, leaving an electron-lucent residual portion of the nucleus (RN). A mitochondrion (Mi) is also associated with the dense portion of the nucleus. Note the electron-dense material beneath the plasmalemma at the base of the protrusions (arrows). F, flagella. Bar = 200 nm. (F) Low power of a mid-stage microgametocyte of *T. gondii* showing a number of microgametes maturing within the parasitophorous vacuole by elongation of the nucleus (N) and mitochondrion (Mi) and growth of the flagella (F) while still attached by their anteriors to the mother cell by a thin neck of cytoplasm with a marked electron-dense collar (arrows). B, basal body. Bar = 1 μm. (G) Stage (similar to that shown in panel E) with immunolabeling for MORN1 showing the electron-dense nucleus (N) protruding into the lumen with adjacent mitochondrion and flagella. Note the gold particles in the collar region of the protruding cytoplasm (arrows) but also in the protruded cytoplasm between the mitochondrion and plasmalemma (arrowhead). RN, residual nucleus. Bar = 100 nm. (H) Part of a maturing microgamete (at a stage similar to that

triolar complex, with daughter formation always associated with the final round of mitosis and initiated directly above each nuclear spindle pole. In the present study, MORN1 appeared to be a unifying feature across the various processes. In all cases, the nuclear poles are labeled with MORN1 as well as the free and growing edge of the conical-shaped IMC, irrespective of whether daughter formation occurs at the surface (classical schizogony) or within the cytoplasm (endodyogeny, *Toxoplasma* endopolygeny, or *Sarcocystis* endopolygeny). The association of MORN1 with the IMC during *Sarcocystis* endopolygeny has previously been described (15). The IMC consists of a double-unit membrane structure formed by flattened vacuoles produced by the Golgi, with an underlying meshwork of intermediate filaments (named IMC proteins) and longitudinally running microtubules (2–4, 28). MORN1 is present as a continuous ring on the posterior end of the IMC, and this location, confirmed by immunoelectron microscopy, is consistent with the "free" end of the IMC, where no microtubules are observed (15). In the final stage, the posterior ring at the point of attachment with the residual body is strongly labeled. In contrast, posterior labeling is reduced in free merozoites. These features are similar to those observed in the sporozoite of *E. tenella* (Fig. 4H).

The loss of intensity upon maturation suggests that MORN1 is required in the budding process but less so to maintain the cytoskeleton in the mature zoite. It was previously shown that in *T. gondii* TgMORN1 segregates in roughly equal proportions in the detergent-soluble and detergent-resistant fractions (15). Since the majority of *T. gondii* TgMORN1 is found at the posterior ring in mature and dividing tachyzoites, these data are consistent with MORN1 having a bridging role between the alveolar vesicles forming the inner membrane and the intermediate filaments of the IMC, specifically at the free end of the IMC. In the case for *P. falciparum* schizogony, Western blotting with the anti-TgMORN1 antibody shows that PfMORN1 is under the level of detection in the early stages of development (ring and trophozoite). This pattern is in agreement with the microarray data (www.plasmodb.org) which indicate low-transcript abundance in early stages and a strong increase, with a peak at 38 h in the 48-h intraerythrocytic cycle (1, 24), coinciding with the initiation of merozoite budding. In addition, detergent extraction showed that the signal is found in both the detergent-soluble and -insoluble fractions, which is comparable to the case for *T. gondii* (15). Therefore, it appears that MORN1 is present in the same functional niche in *T. gondii* and *P. falciparum*, at the interface between alveolar membrane and intermediate filament cytoskeleton. These data support a model wherein TgMORN1 fulfills a bridging position between the alveolar membrane and the IMC-filament meshwork. However, the exact function of the MORN domain is not known. It has been shown that the MORN domain is able to maintain a membrane association through direct binding to phospholipids (25). This observation fits the detergent-extractable fraction of MORN1, whereas the detergent-resistant fraction could serve as the scaffold maintaining the budding ring. With the similarity of expression and location across the Apicomplexa, MORN1 appears to have a conserved role in daughter bud stabilization during asexual development. Because this location is the site where the bud grows, MORN1 potentially serves as a scaffold for the budding machinery. The overexpression of TgMORN1 resulted in incorrect initiation of the daughter buds and an uncoupling of the microtubular skeleton from the IMC skeleton and resulted in unstructured IMC formation (15). Taken together, this strongly suggests that MORN1 is required for the assembly of the IMC skeleton and/or connection with the microtubule skeleton. We previously showed that myosin C is colocalizing with the MORN1 ring during *T. gondii* tachyzoite budding (15), but this may not be the case for other parasites, because myosin C is not strongly conserved across the Apicomplexa (data not shown). More recently, a calcium-dependent contraction of the MORN1 ring in the maturation of the daughters was proposed to be mediated by TgCentrin2 (17). The future direction of our work is to identify the functional components in the establishment and extension of the asexual bud.

Microgamete. Unfortunately there are no in vitro systems for the production of the sexual stages of any coccidian parasite, which has greatly limited the examination of these parasites by molecular techniques. The current study therefore provides a significant extension of current molecular knowledge. We were able to examine the expression and localization of MORN1 during sexual development within the definitive host by using anti-TgMORN1 for four coccidian species (*T. gondii*, *E. acervulina*, *E. tenella*, and *E. maxima*). However, the possibility that anti-TgMORN1 staining in microgametes results from cross-reactivity of the antibody with other MORN domain containing proteins cannot be excluded, although it is unlikely, since the weak 41-kDa band observed by Western blotting was consistent with the predicted mass of EtMORN1.

The role of the MORN1-positive nuclear pole appears to direct to the location of microgamete formation, as discussed above. The formation of a MORN1-positive ring-like structure beneath the plasmalemma is shared between both sexual and asexual development, but in the case of the microgametocyte, MORN1 was associated with amorphous dense material located beneath the plasmalemma in the absence of an IMC. The dense collar at the site of microgamete protrusion has previously been described for various species of *Eimeria*, *Isospora*

shown in panel F), where gold particles can be seen associated with the dense collar underlying the plasmalemma (arrows) and also between the nucleus (N) and mitochondrion (Mi) of the microgamete (arrowhead). Bar = 100 nm. (I) Scanning electron micrograph of a mature microgamete showing the elongated nucleus (N) and the two very long flagella (F). Bar = 500 nm. (J) Longitudinal section through a mature microgamete showing the two flagella (F) arising from basal bodies in the anterior below which is the elongated mitochondrion (Mi) and then the electron-dense nucleus (N). Bar = 500 nm. (K) An immunostained longitudinal section showing a few gold particles anterior (arrowhead) to the basal bodies (B) and a larger number of gold particles lining either side of the mitochondrion (Mi). The gold particles were located between the mitochondrion and the plasmalemma, but they did not appear to encircle the mitochondrion. Bar = 200 nm. (L) Cross section through the anterior portion of a microgamete at the level where the mitochondrion (Mi) and nucleus (N) overlap. Note that the gold particles (arrowheads) only partially surround the mitochondrion. Bar = 100 nm. (M) Detail of the anterior of a microgamete showing a number of gold particles located both apical (arrow) and basal (arrowhead) to the basal body. Bar = 100 nm.

felis, and *T. gondii* (6, 11, 33). It appears that MORN1 is associated with ring formation and maintains the integrity of the site of microgamete budding. This observation suggests that the ring-like appearance of MORN1 requires neither IMC nor microtubules and is controlled at another cytoskeletal level. MORN1 itself could, at least in part, play a role in this, as MORN1 shows a strong tendency to aggregate into multimers and, upon overexpression, has been observed in fiber-like structures (15, 18; N. Sahoo and M. J. Gubbels, unpublished data). Interestingly, an IMC1 knockout generated in *Plasmodium berghei* resulted in sideways budding of sporozoites from the oocyst and mechanically unstable sporozoites (21). It is expected that MORN1 localization is undisturbed in this context, and this will be interesting to investigate.

Since the developing microgamete remained enclosed by the plasmalemma of the mother cell, new membrane is required. New membrane may be formed within the developing microgamete, or it could be an extension of plasmalemma from the mother cell, which may mean movement through the collar region. Since the flagella form by an outgrowth into the parasitophorous vacuole, the subunits for microtubular formation must be transported to the free end of the flagella. Unlike merozoite formation, where there is a budding out involving posterior growth of the pellicle, the developing microgamete remains attached by the anterior end and undergoes changes in shape during maturation while still attached. The maintenance of the connection during microgamete maturation will be important for the rapid movement of materials synthesized in the mother cell into the microgametes. This will be particularly important for the growth of the flagella.

An additional observation is the finding of MORN1-positive material associated with the anterior end of the microgamete located within the apex and also partially enclosing the mitochondrion. This is the first report of a specific molecule associated with microgamete formation and the mature microgamete. Therefore, MORN1 is the first immunocytochemical marker that can be used to identify individual microgametes, which, due to their small size, can be extremely difficult to identify in normal histological sections. It can be hypothesized that this anterior location of MORN1 is involved in maintaining rigidity and structural integrity of the microgamete during massive physical stresses that will be associated with flagellar movement. It may also be that it functions as the anchor of the mitochondria to stay close to the flagellum, where the energy produced in the mitochondria is consumed by the beating flagellum (Fig. 7M). Similar close membrane oppositions have previously been described for eukaryotic myocytes, where a MORN1-like protein called junctophilin maintains the sarcoplasmic reticulum position underlying the plasma membrane (27, 41).

Conclusion. The exact function of the MORN1 protein is unknown, but from the distribution observed in the present study across the Apicomplexa, it is possible to hypothesize about its role. The amount of MORN1 protein appears to vary with developmental stage: an increased amount is associated with daughter and microgamete formation during asexual proliferation and microgametogony, respectively, but it is not observed during macrogametogony, where no division occurs. This distribution during both asexual and sexual development and the location in the mature zoite and microgamete would be consistent with MORN1 maintaining structural integrity, probably by cross-linking other structural components. This may also explain its possible role within the nuclear pole. Further characterization of additional components that specifically interact with MORN1 are under way to advance our understanding of the specific and distinct localizations and roles of MORN1 in the various developmental processes.

ACKNOWLEDGMENTS

This work was supported in part by a Scientist Development Grant from the American Heart Association (no. 0635480N) to M.-J.G. and a Knights Templar Eye Foundation Research Grant to N.S. M.-J.G. is a Smith Family Foundation New Investigator (through the Ludcke Foundation). D.J.P.F. was supported by an equipment grant from the Wellcome Trust.

We thank Damer Blake for access to *E. maxima*-infected chickens.

REFERENCES

1. **Bozdech, Z., M. Llinas, B. L. Pulliam, E. D. Wong, J. Zhu, and J. L. DeRisi.** 2003. The transcriptome of the intraerythrocytic developmental cycle of Plasmodium falciparum. PLoS Biol. **1:**E5.
2. **Dubremetz, J. F.** 1975. Genesis of merozoites in the coccidia, Eimeria necatrix. Ultrastructural study. J. Protozool. **22:**71–84. (In French.)
3. **Dubremetz, J. F.** 1973. Ultrastructural study of schizogonic mitosis in the coccidian, Eimeria necatrix (Johnson 1930). J. Ultrastruct. Res. **42:**354–376. (In French.)
4. **Dubremetz, J. F., and Y. Y. Elsner.** 1979. Ultrastructural study of schizogony of Eimeria bovis in cell cultures. J. Protozool. **26:**367–376.
5. **Ferguson, D. J., S. I. Belli, N. C. Smith, and M. G. Wallach.** 2003. The development of the macrogamete and oocyst wall in Eimeria maxima: immunolight and electron microscopy. Int. J. Parasitol. **33:**1329–1340.
6. **Ferguson, D. J., A. Birch-Andersen, W. M. Hutchison, and J. C. Siim.** 1980. Ultrastructural observations on microgametogenesis and the structure of the microgamete of Isospora felis. Acta Pathol. Microbiol. Scand. Sect. B **88:** 151–159.
7. **Ferguson, D. J., A. Birch-Andersen, W. M. Hutchison, and J. C. Siim.** 1977. Ultrastructural studies on the endogenous development of Eimeria brunetti. II. Microgametogony and the microgamete. Acta Pathol. Microbiol. Scand. Sect. B **85B:**67–77.
8. **Ferguson, D. J., A. Birch-Andersen, W. M. Hutchison, and J. C. Siim.** 1977. Ultrastructural studies on the endogenous development of eimeria brunetti. III. Macrogametogony and the macrogamete. Acta Pathol. Microbiol. Scand. Sect. B **85B:**78–88.
9. **Ferguson, D. J., M. F. Cesbron-Delauw, J. F. Dubremetz, L. D. Sibley, K. A. Joiner, and S. Wright.** 1999. The expression and distribution of dense granule proteins in the enteric (Coccidian) forms of Toxoplasma gondii in the small intestine of the cat. Exp. Parasitol. **91:**203–211.
10. **Ferguson, D. J., F. L. Henriquez, M. J. Kirisits, S. P. Muench, S. T. Prigge, D. W. Rice, C. W. Roberts, and R. L. McLeod.** 2005. Maternal inheritance and stage-specific variation of the apicoplast in *Toxoplasma gondii* during development in the intermediate and definitive host. Eukaryot. Cell **4:**814–826.
11. **Ferguson, D. J., W. M. Hutchison, J. F. Dunachie, and J. C. Siim.** 1974. Ultrastructural study of early stages of asexual multiplication and microgametogony of Toxoplasma gondii in the small intestine of the cat. Acta Pathol. Microbiol. Immunol. Scand. Sect. B **82:**167–181.
12. **Ferguson, D. J., W. M. Hutchison, and J. C. Siim.** 1975. The ultrastructural development of the macrogamete and formation of the oocyst wall of Toxoplasma gondii. Acta Pathol. Microbiol. Scand. Sect. B **83:**491–505.
13. **Ferguson, D. J., S. F. Parmley, and S. Tomavo.** 2002. Evidence for nuclear localisation of two stage-specific isoenzymes of enolase in Toxoplasma gondii correlates with active parasite replication. Int. J. Parasitol. **32:**1399–1410.
14. **Ferguson, D. J. P., S. A. Campbell, F. L. Henriquez, L. Phan, E. Mui, T. A. Richards, S. P. Muench, M. Allary, J. Z. Lu, S. T. Prigge, F. Tomley, M. W. Shirley, D. W. Rice, R. McLeod, and C. W. Roberts.** 2007. Enzymes of type II fatty acid synthesis and apicoplast differentiation and division in Eimeria tenella. Int. J. Parasitol. **37:**33–51.
15. **Gubbels, M. J., S. Vaishnava, N. Boot, J. F. Dubremetz, and B. Striepen.** 2006. A MORN-repeat protein is a dynamic component of the *Toxoplasma gondii* cell division apparatus. J. Cell Sci. **119:**2236–2245.
16. **Hartmann, J., K. Hu, C. Y. He, L. Pelletier, D. S. Roos, and G. Warren.** 2006. Golgi and centrosome cycles in Toxoplasma gondii. Mol. Biochem. Parasitol. **145:**125–127.
17. **Hu, K.** 2008. Organizational changes of the daughter basal complex during the parasite replication of Toxoplasma gondii. PLoS Pathog. **4:**e10.
18. **Hu, K., J. Johnson, L. Florens, M. Fraunholz, S. Suravajjala, C. DiLullo, J. Yates, D. S. Roos, and J. M. Murray.** 2006. Cytoskeletal components of an

invasion machine—the apical complex of Toxoplasma gondii. PLoS Pathog. **2:**121–138.
19. **Hu, K., T. Mann, B. Striepen, C. J. Beckers, D. S. Roos, and J. M. Murray.** 2002. Daughter cell assembly in the protozoan parasite Toxoplasma gondii. Mol. Biol. Cell **13:**593–606.
20. **Jacobs, D., J. F. Dubremetz, A. Loyens, F. Bosman, and E. Saman.** 1998. Identification and heterologous expression of a new dense granule protein (GRA7) from Toxoplasma gondii. Mol. Biochem. Parasitol. **91:**237–249.
21. **Khater, E. I., R. E. Sinden, and J. T. Dessens.** 2004. A malaria membrane skeletal protein is essential for normal morphogenesis, motility, and infectivity of sporozoites. J. Cell Biol. **167:**425–432.
22. **Köhler, S., C. F. Delwiche, P. W. Denny, L. G. Tilney, P. Webster, R. J. Wilson, J. D. Palmer, and D. S. Roos.** 1997. A plastid of probable green algal origin in Apicomplexan parasites. Science **275:**1485–1489.
23. **Kooij, T. W., and K. Matuschewski.** 2007. Triggers and tricks of Plasmodium sexual development. Curr. Opin. Microbiol. **10:**547–553.
24. **Le Roch, K. G., Y. Zhou, P. L. Blair, M. Grainger, J. K. Moch, J. D. Haynes, P. De La Vega, A. A. Holder, S. Batalov, D. J. Carucci, and E. A. Winzeler.** 2003. Discovery of gene function by expression profiling of the malaria parasite life cycle. Science **301:**1503–1508.
25. **Ma, H., Y. Lou, W. H. Lin, and H. W. Xue.** 2006. MORN motifs in plant PIPKs are involved in the regulation of subcellular localization and phospholipid binding. Cell Res. **16:**466–478.
26. **Mann, T., and C. Beckers.** 2001. Characterization of the subpellicular network, a filamentous membrane skeletal component in the parasite Toxoplasma gondii. Mol. Biochem. Parasitol. **115:**257–268.
27. **Minamisawa, S., J. Oshikawa, H. Takeshima, M. Hoshijima, Y. Wang, K. R. Chien, Y. Ishikawa, and R. Matsuoka.** 2004. Junctophilin type 2 is associated with caveolin-3 and is down-regulated in the hypertrophic and dilated cardiomyopathies. Biochem. Biophys. Res. Commun. **325:**852–856.
28. **Nichols, B. A., and M. L. Chiappino.** 1987. Cytoskeleton of Toxoplasma gondii. J. Protozool. **34:**217–226.
29. **Ogino, N., and C. Yoneda.** 1966. The fine structure and mode of division of Toxoplasma gondii. Arch. Ophthalmol. **75:**218–227.
30. **Piekarski, G., B. Pelster, and H. M. Witte.** 1971. Endopolygeny in Toxoplasma gondii. Z. Parasitenkd. **36:**122–130. (In German.)
31. **Radke, J. R., B. Striepen, M. N. Guerini, M. E. Jerome, D. S. Roos, and M. W. White.** 2001. Defining the cell cycle for the tachyzoite stage of Toxoplasma gondii. Mol. Biochem. Parasitol. **115:**165–175.
32. **Schmatz, D. M., M. S. Crane, and P. K. Murray.** 1984. Purification of Eimeria sporozoites by DE-52 anion exchange chromatography. J. Protozool. **31:**181–183.
33. **Scholtyseck, E., H. Mehlhorn, and D. M. Hammond.** 1972. Electron microscope studies of microgametogenesis in Coccidia and related groups. Z. Parasitenkd. **38:**95–131.
34. **Scholtyseck, E., H. Mehlhorn, and D. M. Hammond.** 1971. Fine structure of macrogametes and oocysts of Coccidia and related organisms. Z. Parasitenkd. **37:**1–43.
35. **Sheffield, H. G., and M. L. Melton.** 1968. The fine structure and reproduction of Toxoplasma gondii. J. Parasitol. **54:**209–226.
36. **Shirley, M. W.** 1995. Eimeria species and strains of chickens, p. 1–24. *In* J. Eckert, R. Braun, M. W. Shirley, and P. Coudert (ed.), Biotechnology—guidelines on techniques in coccidiosis research. The European Commission DGXII, Luxembourg, Luxembourg.
37. **Sinden, R. E.** 1983. The cell biology of sexual development in plasmodium. Parasitology **86:**7–28.
38. **Speer, C. A., and J. P. Dubey.** 1981. An ultrastructural study of first- and second-generation merogony in the coccidian Sarcocystis tenella. J. Protozool. **28:**424–431.
39. **Striepen, B., M. J. Crawford, M. K. Shaw, L. G. Tilney, F. Seeber, and D. S. Roos.** 2000. The plastid of Toxoplasma gondii is divided by association with the centrosomes. J. Cell Biol. **151:**1423–1434.
40. **Striepen, B., C. N. Jordan, S. Reiff, and G. G. van Dooren.** 2007. Building the perfect parasite: cell division in apicomplexa. PLoS Pathog. **3:**e78.
41. **Takeshima, H., S. Komazaki, M. Nishi, M. Iino, and K. Kangawa.** 2000. Junctophilins: a novel family of junctional membrane complex proteins. Mol. Cell **6:**11–22.
42. **Trager, W., and J. B. Jensen.** 2005. Human malaria parasites in continuous culture. 1976. J. Parasitol. **91:**484–486.
43. **Vaishnava, S., D. P. Morrison, R. Y. Gaji, J. M. Murray, R. Entzeroth, D. K. Howe, and B. Striepen.** 2005. Plastid segregation and cell division in the apicomplexan parasite Sarcocystis neurona. J. Cell Sci. **118:**3397–3407.
44. **Wallach, M., N. C. Smith, M. Petracca, C. M. Miller, J. Eckert, and R. Braun.** 1995. Eimeria maxima gametocyte antigens: potential use in a subunit maternal vaccine against coccidiosis in chickens. Vaccine **13:**347–354.